



## PLANE STRAIN NEAR-TIP FIELDS FOR ELASTIC- PLASTIC INTERFACE CRACKS

XIAOMIN DENG

Department of Mechanical Engineering, University of South Carolina, Columbia, SC 29208,  
U.S.A.

(Received 24 September 1993; in revised form 18 August 1994)

**Abstract**—The plane strain problem of a stationary interface crack between two dissimilar ductile solids is studied asymptotically, where the ductile solids are assumed to be incompressible, elastic-perfectly plastic, and obey the  $J_2$ -flow theory of plasticity. Candidate asymptotic crack-tip assemblies of plastic and elastic sectors are proposed, and all associated admissible near-tip fields are presented. It is found that when the crack tip is fully surrounded by plastic sectors, then only isolated, mode I type solutions exist. When an elastic sector appears along the crack flank in one solid and all other sectors in the two solids are plastic, a two-parameter family of solutions exists, which produces crack-tip stress variations similar to those of the mixed-mode as well as mode I slip-line fields for homogeneous ductile materials. When each of the two solids contains an elastic sector along the crack flank, the crack-tip solutions are found to belong to a four-parameter family, which also resembles mixed-mode and mode I solutions for homogeneous solids. For completeness, the special case of ductile/rigid interfaces is also studied, and several one-parameter families of crack-tip solutions are obtained, which are complementary to those already published in the literature.

### INTRODUCTION

Interface cracks exist in many engineering materials and structures. For example, they can be found in composite materials, along welded or bonded joints, or between the case and the core of case-hardened machine components. The overall strength and toughness of these materials and structures depend very much on the behavior of the interface cracks and the toughness of the interface and the component materials. An important and integral part of the process of characterizing the crack behavior is the analysis of the crack-tip stress and deformation fields.

In the analysis of interface cracks, the linear theory of elasticity has played a pioneering role and is still the leading method for studying interfacial fracture in solids. For a summary of research work in this area the reader is referred to a recent review article by Hutchinson and Suo (1992). During the last few years, the theory of plasticity has been emerging as an important analysis tool for cases where the assumption of elasticity breaks down, or when an understanding of crack-tip inelastic behavior is necessary, for example, for many metal-matrix composite materials. Studies in this area have been led by the finite element analyses of Shih and Asaro (1988, 1989), and cover a variety of cases, including stationary and propagating cracks, hardening and ideally plastic solids, out-of-plane and in-plane deformations, first-order and higher-order analyses, and cracks with and without contact zones. One emphasis of these studies has been on interface cracks in power-law hardening materials, with an eye towards HRR-like variable separable crack-tip solutions (e.g. Shih and Asaro, 1988, 1989; Gao and Lou, 1990; Wang, 1990; Champion and Atkinson, 1990, 1991; Aravas and Sharma, 1991; Sharma and Aravas, 1991, 1993). Another emphasis has been placed on interface cracks between an elastic-perfectly plastic material and a rigid substrate, partly because the mathematics involved is less demanding than in the case of ductile/ductile interfacial cracks, and partly because the resulting solutions are quite revealing and interesting by themselves (e.g. Guo and Keer, 1990; Zywicki and Parks, 1990, 1992; Ponte Castaneda and Mataga, 1991; Drugan, 1991). Dynamic crack growth along interfaces between an ideally plastic solid and a rigid substrate and between two dissimilar ideally plastic solids is studied by Deng (1993).

In the current investigation, attention is called to the plane strain problem of a stationary interface crack between two dissimilar ductile solids, which are taken to be incompressible, ideally plastic, and satisfy the von Mises yield condition and the associated flow rule. The purpose here is to study the mathematical structure of the asymptotic stress field around the interface crack in terms of a variety of admissible crack-tip assemblies of plastic as well as elastic sectors. The asymptotic crack-tip solutions presented in this paper bear some similarity to those of the finite element studies by Shih and Asaro (1988, 1989) for power-law hardening bimetals, and possess many features found in mixed-mode crack-tip fields in homogeneous, ideally plastic solids obtained by Dong and Pan (1990). For completeness, interface cracks between an ideally plastic solid and a rigid substrate is also addressed, with some new solutions obtained. The results of this study, together with the findings of Guo and Keer (1990) and Zywicki and Parks (1992), form a more complete picture about the asymptotic features of the stationary interfacial crack-tip fields in elastic-perfectly plastic bimetals.

#### MATHEMATICAL FORMULATION

For the purpose of asymptotic analysis, we consider a straight, stationary, semi-infinite crack along the interface of material 1, occupying the upper half-plane, and material 2, occupying the lower half-plane, as illustrated in Fig. 1. In this study, material 1 will always be ductile, meaning that it is ideally plastic, and obeys the  $J_2$ -flow theory of plasticity, and material 2 will be either rigid or ductile. For simplicity, we will consider incompressible materials only.

The governing equations in plane strain for a generic ductile material specified above are briefly outlined here. With reference to the rectangular Cartesian coordinate system in Fig. 1, the equilibrium equations are given by

$$\sigma_{\alpha\beta,\beta} = 0 \quad (1)$$

where  $\sigma_{\alpha\beta}$  (Greek indices have range 1 and 2) are the in-plane components of the stress tensor, with summation convention in indicial notation adopted, and  $()_{,\beta} = \partial()/\partial x_\beta$ , with  $x_1 = x$  and  $x_2 = y$ . The relations between the components of the strain tensor,  $\varepsilon_{\alpha\beta}$ , and those of the displacement vector,  $u_{\alpha s}$ , are

$$\varepsilon_{\alpha\beta} = (u_{\alpha,\beta} + u_{\beta,\alpha})/2. \quad (2)$$

Due to incompressibility, the constitutive law for the ductile material can be written as

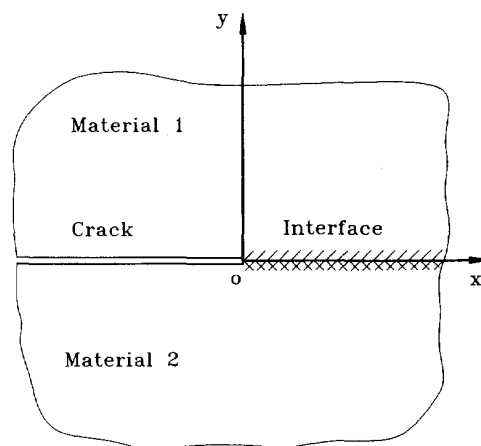


Fig. 1. A stationary crack along a bimaterial interface.

$$\dot{\epsilon}_{\alpha\beta} = (1/2\mu)\dot{s}_{\alpha\beta} + \lambda s_{\alpha\beta} \quad (3)$$

where  $\mu$  is the elastic shear modulus, and a superimposed dot denotes a material time derivative. The flow factor  $\lambda$  is non-negative in a plastic state and identically zero in an elastic state, and  $s_{\alpha\beta} = \sigma_{\alpha\beta} - \sigma\delta_{\alpha\beta}$  is the component of the deviatoric stress tensor, where  $\sigma = \sigma_{ii}/3$  (Latin indices have range 1, 2, 3) is the mean or hydrostatic stress and  $\delta_{\alpha\beta}$  is the Kronecker delta. From the plane strain requirement  $u_3 = \epsilon_{3i} = \sigma_{3\beta} = 0$  and the incompressibility of the material, we find that

$$u_{\alpha,z} = 0; \quad \sigma = \sigma_{\alpha\alpha}/2 = \sigma_{33}; \quad s_{11} = -s_{22} = (\sigma_{11} - \sigma_{22})/2, \quad s_{33} = 0 \quad (4)$$

from which the von Mises yield condition can be expressed as

$$s_{22}^2 + s_{12}^2 = k^2 \quad (5)$$

where constant  $k$  is the material's yield stress in pure shear.

The above governing equations must be supplemented by traction and displacement continuity conditions across the interface and by the traction-free boundary conditions along the crack surfaces. When material 2 is taken to be rigid, the continuity conditions along the interface are in the form of zero displacements, and consequently, the tractions along the interface are not restricted.

#### ASYMPTOTIC SOLUTIONS FOR INDIVIDUAL SECTORS

To facilitate the asymptotic analysis at the crack tip, we make the following simplifying assumptions: (a) the mean or hydrostatic stress is bounded near the crack tip, (b) the crack tip region is composed of wedge-shaped sectors separated by radial lines from the crack tip, (c) within each crack-tip sector, the stresses are uniformly convergent as the crack tip is approached. Under such assumptions, it can be argued that as the crack tip is approached, the stresses in each sector can be treated as functions of the angular position only. As such, and in terms of the polar stress components  $\sigma_{rr}$ ,  $\sigma_{\theta\theta}$ ,  $\sigma_{r\theta}$ , where  $(r, \theta)$  are the crack-tip polar coordinates associated with the  $x$ - $y$  coordinate system, the equilibrium equations in (1) can be reduced to:

$$\begin{aligned} \sigma_{rr} - \sigma_{\theta\theta} + d\sigma_{rr}/d\theta &= 0, \\ 2\sigma_{r\theta} + d\sigma_{\theta\theta}/d\theta &= 0 \end{aligned} \quad (6)$$

where  $r \rightarrow 0$ . Similarly, in terms of the polar stress components, the yield condition in eqn (5) can be written as

$$\left(\frac{\sigma_{rr} - \sigma_{\theta\theta}}{2}\right)^2 + \sigma_{r\theta}^2 = k^2 \quad (7)$$

which can be differentiated with respect to  $\theta$ , and can be used to derive,

$$(\sigma_{rr} - \sigma_{\theta\theta}) \frac{d\sigma}{d\theta} = 0 \quad (8)$$

where again  $\sigma$  is the mean stress and equals  $(\sigma_{rr} + \sigma_{\theta\theta})/2$  for incompressible solids.

Equations (6) and (8), subjected to eqn (7), involve exactly three unknowns and are sufficient to produce elastic-plastic solutions for crack-tip plastic sectors. It can be shown (see, for example, Rice, 1982; Dong and Pan, 1990) that there are two types of solutions, each corresponding to one type of plastic sector. In terms of terminology used in slip-line field theory, the first type of solution is for a *uniform or constant stress plastic sector*, which

comes from  $d\sigma/d\theta = 0$  in eqn (8), and the second type is for a *centered fan plastic sector*, which derives from  $(\sigma_{rr} - \sigma_{\theta\theta}) = 0$  in eqn (8).

In a uniform plastic sector, the rectangular stress components are all constant, and the stress state can be represented by the constant mean stress,  $\sigma_0$ , and a constant angle  $\psi_0$ , as

$$\left. \begin{aligned} \sigma_{11} &= \sigma_0 - k \cos \psi_0 \\ \sigma_{22} &= \sigma_0 + k \cos \psi_0 \\ \sigma_{12} &= k \sin \psi_0 \end{aligned} \right\} \text{ or } \left. \begin{aligned} \sigma_{rr} &= \sigma_0 - k \cos (2\theta + \psi_0) \\ \sigma_{\theta\theta} &= \sigma_0 + k \cos (2\theta + \psi_0) \\ \sigma_{r\theta} &= k \sin (2\theta + \psi_0) \end{aligned} \right\}. \tag{9}$$

In a centered fan plastic sector, the stress state is given by

$$\left. \begin{aligned} \sigma_{11} &= \sigma_* - (\pm)k (2\theta + \sin 2\theta) \\ \sigma_{22} &= \sigma_* - (\pm)k (2\theta - \sin 2\theta) \\ \sigma_{12} &= (\pm)k \cos 2\theta \end{aligned} \right\} \text{ or } \left. \begin{aligned} \sigma_{rr} &= \sigma_* - (\pm)2k\theta \\ \sigma_{\theta\theta} &= \sigma_* - (\pm)2k\theta \\ \sigma_{r\theta} &= (\pm)k \end{aligned} \right\} \tag{10}$$

where  $\sigma_*$  is a constant. There are two options in eqn (10), as indicated by the choice of a + or - sign.

Besides the two types of plastic sectors listed above, there is also the possibility of elastic sectors around the crack tip. As shown by Dong and Pan (1990), the stress state in an elastic sector can be written as

$$\begin{aligned} \sigma_{11} &= 2a + 2b\theta + b \sin 2\theta - 2c \\ \sigma_{22} &= 2a + 2b\theta - b \sin 2\theta + 2c \\ \sigma_{12} &= -b \cos 2\theta - 2d \end{aligned} \tag{11}$$

where  $a, b, c, d$  are constants.

To obtain a complete solution for the crack tip stress state, the various sectors discussed above must be assembled in a proper order so as to satisfy all inter-sector continuity conditions as well as boundary conditions along the interface and the crack surfaces. In this study, we only look for solutions that have full inter-sector stress continuities within each of the two component materials. Presented in the following are candidate assemblies of crack-tip sectors that satisfy the preceding specifications. To distinguish between solutions for the two dissimilar materials of ductile/ductile interfaces, many quantities for the upper half-plane will be denoted with subscript + while those for the lower half-plane with subscript -.

DUCTILE/RIGID INTERFACE: TYPE I ASSEMBLY

We consider the case of a ductile solid atop a rigid substrate. As shown in Fig. 2, the crack-tip region in the top half-plane can be divided into three sectors—two uniform sectors, one bordering the interface and the other along the crack flank, as indicated by the letter *U*, and one centered fan sector in between, as indicated by the letter *F*. This assembly is not considered by Guo and Keer (1990) because of the concern that the interface must be a slip line. This concern, however, can be safely waived if we notice that in a uniform

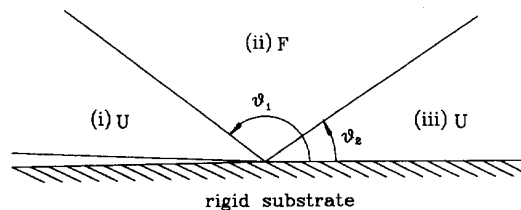


Fig. 2. The type I assembly of sectors around a ductile/rigid interface crack.

sector the strains are in general nonsingular (Rice and Tracey, 1973). Since the strains are finite in a uniform sector, the materials there are not necessarily deforming rigid-plastically, hence the conclusion that the boundary between a rigid and a rigid-plastically deforming region must be a characteristic need not be applied here. As such, the assembly shown in Fig. 2 is a viable one.

Stress distributions for this assembly belong to two one-parameter families of solutions, which can be grouped together in one set of expressions but used with the choice of a + or - sign. In the following, the stress state in each of the sectors are given sometimes in terms of rectangular components and sometimes in terms of polar components, depending on brevity and convenience. In sector (i) ( $\pi \geq \theta \geq \theta_1$ ):

$$\sigma_{11} = (\pm)2k, \quad \sigma_{12} = \sigma_{22} = 0. \quad (12)$$

In sector (ii) ( $\theta_1 \geq \theta \geq \theta_2$ ):

$$\sigma_{rr} = \sigma_{\theta\theta} = (\pm)k(1 + 3\pi/2 - 2\theta), \quad \sigma_{r\theta} = (\pm)k. \quad (13)$$

In sector (iii) ( $\theta_2 \geq \theta \geq 0$ ):

$$\begin{aligned} \sigma_{11} &= (\pm)k(1 + \pi + \eta - \cos \eta) \\ \sigma_{22} &= (\pm)k(1 + \pi + \eta + \cos \eta) \\ \sigma_{12} &= (\pm)k \sin \eta. \end{aligned} \quad (14)$$

In the above expressions,  $\eta$  ( $-\pi < \eta < \pi/2$ ) is the free parameter for these two families of solutions. The angles separating the sectors are  $\theta_1$  and  $\theta_2$  and are given by

$$\theta_1 = 3\pi/4, \quad \theta_2 = \pi/4 - \eta/2. \quad (15)$$

At the moment, explicit finite element solutions for the case considered here are very limited in the literature, which makes direct comparison difficult. The study by Zywicki and Parks (1992) considered only the small-scale yielding loading case, which does not cover many other loading and geometric conditions that might influence the crack tip stress state (see Larsson and Carlsson, 1973; Rice, 1974). In light of this, we will compare the asymptotic solution here with the results of a finite element study by Shih and Asaro (1988), in which the problem of an interface crack between a Ramberg-Osgood hardening material and a rigid substrate under remote uniform tensile loading is treated. For the weak hardening case with hardening exponent  $n = 10$ , the finite element solution shown in Fig. 12(e) of the original paper by Shih and Asaro (this figure is not repeated here) can be reasonably compared with the solution given here for  $\eta = -3\pi/7$  (Fig. 3) with a + sign in eqns (12)

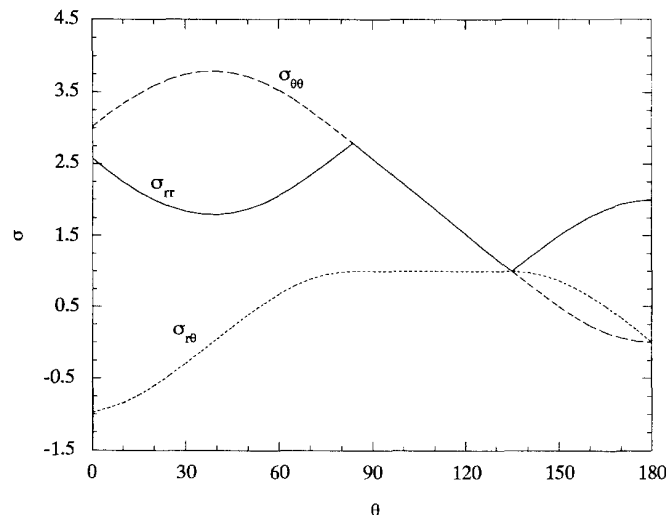


Fig. 3. Crack-tip angular stress variations for the type I assembly of sectors around a ductile/rigid interface crack, normalized by  $k$ , with  $\eta = -3\pi/7$ .

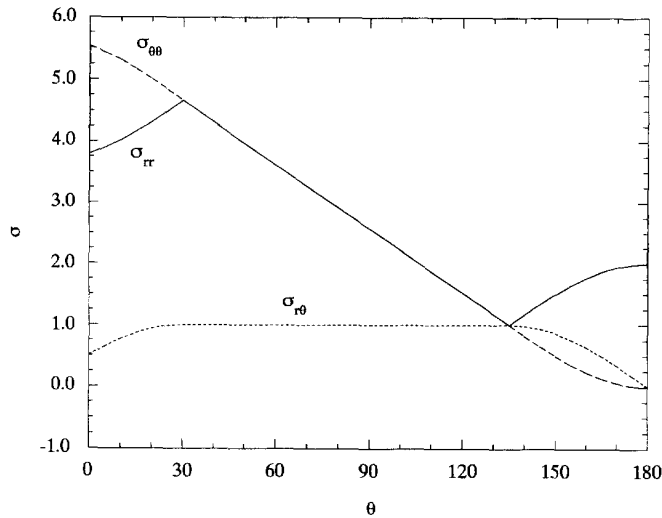


Fig. 4. Crack-tip angular stress variations for the type I assembly of sectors around a ductile/rigid interface crack, normalized by  $k$ , with  $\eta = \pi/6$ .

through (14). The similarity between the two solutions is quite clear. Shown in Fig. 4 are the stress distributions for the case of  $\eta = \pi/6$ , also with a + sign, which very much resemble those of the classic slip-line solution for the mode I crack-tip field. Note that all stress quantities shown in the figures in this and subsequent sections are normalized by the pure shear yielding stress  $k$  of the upper material.

DUCTILE/RIGID INTERFACE: TYPE II ASSEMBLY

As shown in Fig. 5, this assembly is built on the previous one by adding a centered fan plastic sector (iv) between the bimaterial interface and the uniform plastic sector (iii). Again, two families of solutions exist and they can be represented in one set of expressions with the choice of a + or - sign. In sectors (i) through (iii), stresses are still given by eqns (12) through (14), and in sector (iv), they are described by

$$\sigma_{rr} = \sigma_{\theta\theta} = (\pm)k(1 + 3\pi/2 + 2\theta + 2\eta), \quad \sigma_{r,\theta} = -(\pm)k. \tag{16}$$

The free parameter  $\eta$  here is restricted in the interval  $(-\pi, -\pi/2)$ . The angles  $\theta_1$  and  $\theta_2$  are still expressed by eqn (15), and  $\theta_3$  is equal to  $(\theta_2 - \pi/2)$  or  $(-\pi/4 - \eta/2)$ . We note that when the + sign is chosen, the above equations are equivalent to those given by Guo and Keer (1990).

A strong feature of this assembly is that the stress state along the interface always has a non-negligible shear component of  $\sigma_{12} = -(\pm)k$ . When the free parameter  $\eta$  is properly chosen, the above equations can be used to generate stress distributions similar to those of the classic mode II slip-line field, where the shear stress is dominant along the interface. A concern about mode II type fields is that crack surface contact may exist near the crack tip in the elastic region surrounding the crack-tip plastic zone, which may render the solutions

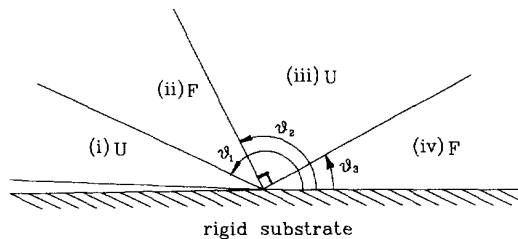


Fig. 5. The type II assembly of sectors around a ductile/rigid interface crack.

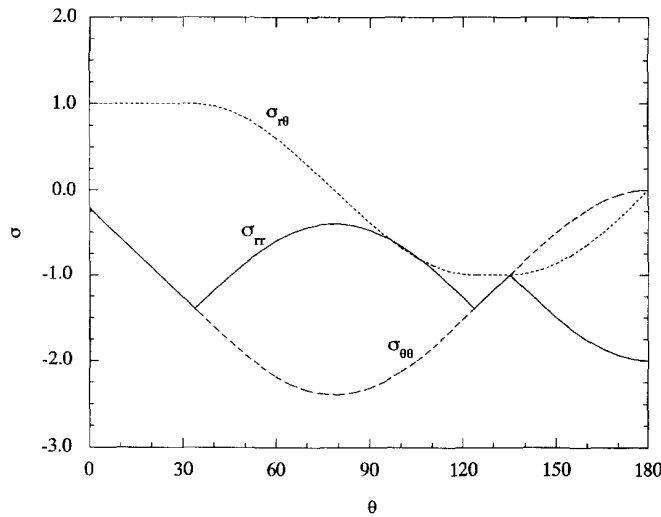


Fig. 6. Crack-tip angular stress variations for the type II assembly of sectors around a ductile/rigid interface crack, normalized by  $k$ , with  $\eta = -7\pi/8$ .

above inapplicable. It appears however, that the above concern can be put aside if the  $-$  sign in the equations is chosen. Obviously, this can be argued from the simple fact that when the bimaterial is incompressible, as it is here, crack surface contact in the elastic region will not occur in a shear field under plane strain conditions. A more important yet less apparent reason is that, when the  $-$  sign is chosen, the shear stress along the interface is positive, as shown, for example, in Fig. 6 for the case  $\eta = -7\pi/8$ . Since, in this mode II type field with positive shear along the interface, the contact zone will be negligibly small if the upper half-plane is purely elastic (incompressible or not) while the lower half is rigid, as indicated by the analysis of Comninou (1978), among others, it is plausible that the same will be true if the elastic material is allowed to yield near the crack tip. In short, when the  $-$  sign is chosen, a mode II type slip-line field may be achievable in practice.

DUCTILE/DUCTILE INTERFACE: ISOLATED SOLUTION

Ductile/ductile interfaces exist in many engineering materials and structures, such as metal-matrix composites and welded joints. Stress states around crack tips along such interfaces have special characteristics and, under certain conditions, can be revealed asymptotically, which will be the emphasis of this paper, as demonstrated in this and the next two sections.

The first crack-tip assembly, as shown in Fig. 7, is composed of plastic sectors only. In either half-plane, a uniform sector exists along the interface, another along the crack flank, and a centered fan will lie between these two. The subscripts  $+$  and  $-$  are used to denote quantities for the upper and lower half-planes respectively. It turns out that no

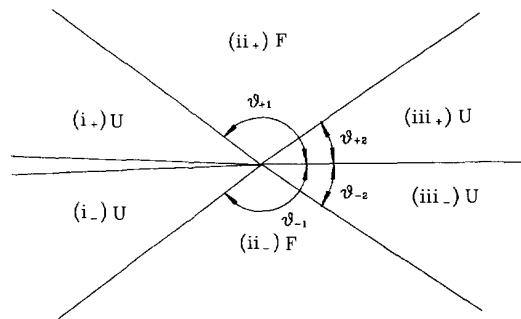


Fig. 7. An assembly of sectors around a ductile/ductile interface crack.

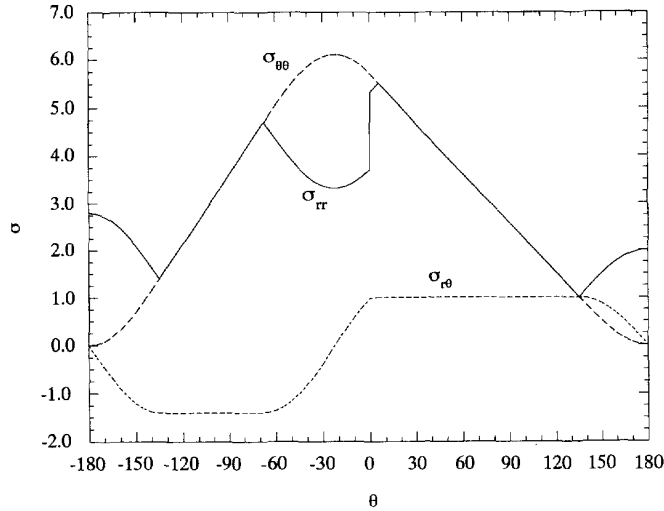


Fig. 8. Crack-tip angular stress variations for the assembly of sectors around a ductile/ductile interface crack shown in Fig. 7, normalized by  $k_+$ , with  $k_+/k_- = 1.0/1.4$ ,  $\eta_- = 1.373$ ,  $\eta_+ = -2.366$ .

families of solutions exist for such an assembly. However, for certain bimetals, two *isolated* solutions can be found for given ratios of  $k_+$  and  $k_-$ , the pure shear yield stresses of the upper and lower materials respectively. In sectors (i<sub>+</sub>) through (iii<sub>+</sub>), expressions for the stresses and angles are identical to those in eqns (12) through (15), except that subscript + must be attached to  $k$ ,  $\eta$ , and the angles separating the sectors, and that  $\eta_+$  is now restricted in the interval  $(-\pi, \pi/2)$ . In sector (i<sub>-</sub>), the stresses are given by

$$\sigma_{11} = (\pm)2k_-, \quad \sigma_{12} = \sigma_{22} = 0. \quad (17)$$

In sector (ii<sub>-</sub>):

$$\sigma_{rr} = \sigma_{\theta\theta} = (\pm)k_-(1 + 3\pi/2 + 2\theta), \quad \sigma_{r\theta} = -(\pm)k. \quad (18)$$

In sector (iii<sub>-</sub>):

$$\begin{aligned} \sigma_{11} &= (\pm)k_-(1 - \eta_- + \cos \eta_-) \\ \sigma_{22} &= (\pm)k_-(1 - \eta_- - \cos \eta_-) \\ \sigma_{12} &= -(\pm)k_- \sin \eta_- \end{aligned} \quad (19)$$

where  $\eta_-$  is limited in the range  $(-3\pi/2, 0)$ . Finally, the angles separating the sectors in the lower half-plane are:

$$\theta_{-1} = -3\pi/4, \quad \theta_{-2} = -3\pi/4 - \eta_-/2. \quad (20)$$

The parameters  $\eta_+$ , for the upper half-plane, and  $\eta_-$ , for the lower half-plane, are not arbitrary—they must be solved from the traction continuity conditions across the interface at  $\theta = 0$ , which are given by

$$\begin{aligned} k_+ \sin \eta_+ &= -k_- \sin \eta_- \\ k_+(1 + \pi + \eta_+ + \cos \eta_+) &= k_-(1 - \eta_- - \cos \eta_-). \end{aligned} \quad (21)$$

This is a set of nonlinear equations and is found to have solutions only when  $k_+$  and  $k_-$  are not greatly different. For example, when  $k_+ = k_-$ , it is found that  $\eta_+ = 0$  and  $\eta_- = -\pi$ , which recovers the mode I slip-line solution for plane strain if the plus sign is chosen in the stress expressions. Similarly, when  $k_+/k_- = 1.0/1.4$ , it is found that  $\eta_+ = 1.373$  and  $\eta_- = -2.366$ . When the plus sign is chosen again, the resulting stress variations (normalized by  $k_+$ ) still resemble those of the mode I slip-line field (see Fig. 8). As such, it appears that



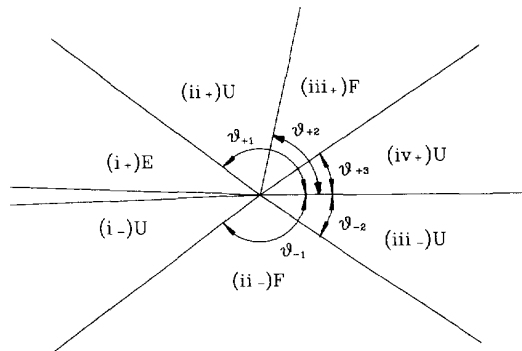


Fig. 9. An assembly of sectors around a ductile/ductile interface crack.

this assembly of sectors is most fitted to cases where the upper and lower ductile materials are only slightly different and are subjected to dominant tensile loadings.

In the following two sections, mixed-mode type stress distributions will be obtained by adding elastic sectors in the crack-tip assembly. Because of the flexibility offered by the existence of elastic sectors around the crack tip, and because of the mixed-mode nature of interfacial crack-tip fields in elastic and hardening elastic-plastic bimetals, the solutions represented by the assemblies proposed below are believed to be more practical and may have a large range of applicability. Also because of the elastic sectors, the asymptotic crack-tip fields will contain several free parameters that can only be determined through full-field solutions, such as those obtained using the finite element methods.

DUCTILE/DUCTILE INTERFACE: TWO-PARAMETER FAMILY OF SOLUTIONS

The crack tip assembly of sectors is illustrated in Fig. 9, where *E* stands for elastic sectors, *U* for uniform plastic sectors, and *F* for centered fan plastic sectors. In this assembly, only one elastic sector is introduced, which resides, without loss of generality, in the upper material. One family of solutions can be found for this assembly, which is controlled by two free parameters,  $T_+$  and  $\theta_{+1}$ , where  $T_+$  equals half of the tensile (or compressive) stress along the crack flank ( $\theta = 180^\circ$ ) in the direction of the *x*-axis, and  $\theta_{+1}$  is the angle separating the elastic sector from the plastic sectors. These two parameters are chosen because their values for a particular problem can be relatively easily identified from a full-field numerical solution. By definition, it is required that  $-k_+ < T_+ < k_+$  and  $0 < \theta_{+1} < \pi$ .

For the upper half-plane, the stresses in sector (i<sub>+</sub>) are given by

$$\begin{aligned} \sigma_{11} &= 2T_+ + 2b_+(\theta - \pi) + b_+ \sin 2\theta \\ \sigma_{22} &= 2b_+(\theta - \pi) - b_+ \sin 2\theta \\ \sigma_{12} &= b_+(1 - \cos 2\theta). \end{aligned} \tag{22}$$

The intermediate parameter  $b_+$  in the above equation is determined by

$$b_+ = \frac{-2T_+ \sin 2\theta_{+1} + \Delta_+}{4(1 - \cos 2\theta_{+1})} \quad \text{or} \quad \frac{-2T_+ \sin 2\theta_{+1} - \Delta_+}{4(1 - \cos 2\theta_{+1})} \tag{23}$$

where

$$\Delta_+ = \sqrt{8(1 - \cos 2\theta_{+1})k_+^2 - 4(1 - \cos 2\theta_{+1})^2 T_+^2}. \tag{24}$$

The choice of  $b_+$  in eqn (23) should be made such that the *effective stress*  $\sigma_{\text{eff}}$ , defined here as

$$\sigma_{\text{eff}} = \sqrt{(1/4)(\sigma_{11} - \sigma_{22})^2 + \sigma_{12}^2} \quad (25)$$

is no greater than the shear yielding stress  $k_+$  for  $\pi \geq \theta \geq \theta_{+1}$ , and that  $|b_+/k_+|(1 - \cos 2\theta_{+1}) < 1$ . Stresses in sector (ii<sub>+</sub>) can be obtained from those in eqn (22) by setting  $\theta$  to  $\theta_{+1}$ .

In sector (iii<sub>+</sub>):

$$\begin{aligned} \sigma_{11} &= T_+ + 2b_+(\theta_{+1} - \pi) \pm k_+(2\theta_{+2} - 2\theta - \sin 2\theta) \\ \sigma_{22} &= T_+ + 2b_+(\theta_{+1} - \pi) \pm k_+(2\theta_{+2} - 2\theta + \sin 2\theta) \\ \sigma_{12} &= \pm k_+ \cos 2\theta. \end{aligned} \quad (26)$$

In sector (iv<sub>+</sub>):

$$\begin{aligned} \sigma_{11} &= \sigma_{+0} - k_+ \cos \eta_+ \\ \sigma_{22} &= \sigma_{+0} + k_+ \cos \eta_+ \\ \sigma_{12} &= k_+ \sin \eta_+ \end{aligned} \quad (27)$$

where  $\sigma_{+0}$  is the (constant) mean stress in sector (iv<sub>+</sub>), which is given by

$$\sigma_{+0} = T_+ + 2b_+(\theta_{+1} - \pi) \pm 2k_+(\theta_{+2} - \theta_{+3}). \quad (28)$$

The angle  $\theta_{+3}$  is related to  $\eta_+$  through

$$\theta_{+3} = -\eta_+/2 \pm \pi/4 \quad (29)$$

and the angle  $\theta_{+2}$  must be determined by satisfying the following two conditions simultaneously:

$$\begin{aligned} \pm k_+ \cos 2\theta_{+2} &= b_+(1 - \cos 2\theta_{+1}) \\ \pm k_+ \sin 2\theta_{+2} &= -T_+ - b_+ \sin 2\theta_{+1}. \end{aligned} \quad (30)$$

For the lower half-plane, the stresses and angles are still given by eqns (17) through (20). The stress states for the upper and lower half-planes must be such that the traction continuity conditions across the interface are satisfied. These conditions can be written as

$$\begin{aligned} \sigma_{+0} + k_+ \cos \eta_+ &= (\pm)k_-(1 - \eta_- - \cos \eta_-) \\ k_+ \sin \eta_+ &= -(\pm)k_- \sin \eta_- \end{aligned} \quad (31)$$

where  $\sigma_{+0}$  is given in eqn (28) and depends, through eqn (29), on  $\eta_+$ . The unknown values for  $\eta_+$  ( $\pm\pi/2 - 2\theta_{+2} \leq \eta_+ \leq \pm\pi/2$ ) and  $\eta_-$  ( $-3\pi/2 \leq \eta_- \leq 0$ ) must be obtained by solving eqns (31) simultaneously. It is noted that, while it is free to choose the + or - sign in front of  $k_-$ , those for the upper material, namely those in eqns (26) through (30) as well as for the interval of  $\eta_+$ , must be determined as part of the solution. Consequently, eqns (31) are rather nonlinear.

To demonstrate that a family of solutions does exist for this crack-tip assembly, results for the case of a bimaterial with  $k_+/k_- = 1.0/0.8$  are illustrated here. (It is noted that the preceding ratio value for  $k_+/k_-$ , and those used earlier and later, are in the ball park of those found between the weld metal and the base metal for welded joints.) Shown in Figs

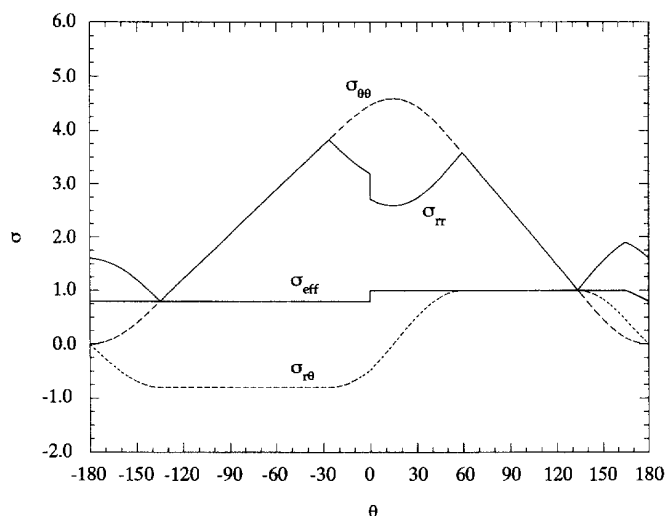


Fig. 10. Crack-tip angular stress variations for the assembly of sectors around a ductile/ductile interface crack shown in Fig. 9, normalized by  $k_+$ , with  $k_+/k_- = 1.0/0.8$ ,  $T_+ = 0.8$ ,  $\theta_{+1} = 165^\circ$ .

10 and 11 are the angular variations of the crack-tip polar stress components and the effective stress  $\sigma_{\text{eff}}$ , all normalized by the shear yielding stress  $k_+$  of the upper material, for two particular cases, both with a  $-$  sign chosen in front of  $k_-$  in the stress equations. Figure 10 is for the case of  $T_+ = 0.8$  and  $\theta_+ = 165^\circ$ , for which it is found from eqn (31) that  $\eta_+ = -0.5032$  and  $\eta_- = -3.789$ . The stress state in this case is seen to resemble that of the classic mode I slip-line field. Figure 11 is for the case of  $T_+ = -0.8$  and  $\theta_+ = 140^\circ$ , for which  $\eta_+ = 0.2034$  and  $\eta_- = -2.886$ . The stress state is similar to that of a mixed-mode crack-tip field shown by, for example, Dong and Pan (1990). (The reader is reminded that the stresses here are normalized by  $k_+$ , and that the effective stress,  $\sigma_{\text{eff}}$ , defined in this paper is equal to the shear yielding stress rather than the tension yielding stress used by Dong and Pan (1990), which results in a small difference in the value of  $\sigma_{\text{eff}}$ .) The elastic sector in the upper half-plane is indicated by the less-than-unity  $\sigma_{\text{eff}}$  value near  $\theta = 180^\circ$ .

DUCTILE/DUCTILE INTERFACE: FOUR-PARAMETER FAMILY OF SOLUTIONS

In the previous assembly, only one elastic sector is introduced, which is motivated by observations from the homogeneous case. To cover the possibility of elastic sectors in both

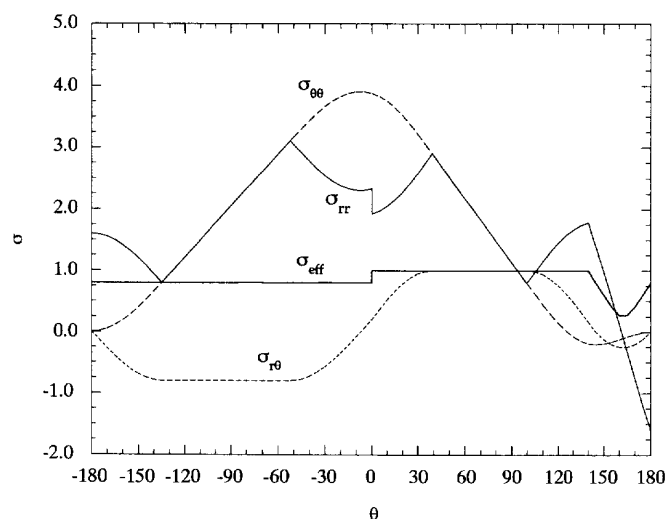


Fig. 11. Crack-tip angular stress variations for the assembly of sectors around a ductile/ductile interface crack shown in Fig. 9, normalized by  $k_+$ , with  $k_+/k_- = 1.0/0.8$ ,  $T_+ = -0.8$ ,  $\theta_{+1} = 140^\circ$ .

half-planes, which might be created due to the mismatch of material properties between the upper and lower half-planes, the crack tip assembly shown in Fig. 12 is proposed here. This assembly can be generated from that in Fig. 9 by adding an elastic sector along the crack flank in the lower half-plane. As a result, a four-parameter family of solutions for the crack-tip stress field can be obtained. The four parameters are  $T_+$  ( $-k_+ < T_+ < k_+$ ) and  $T_-$  ( $-k_- < T_- < k_-$ ), which equal half of the tensile (or compressive) normal stresses along the crack flank at, respectively,  $\theta = +180^\circ$  and  $-180^\circ$  in the direction of the  $x$ -axis, and  $\theta_{+1}$  ( $0 < \theta_{+1} < \pi$ ) and  $\theta_{-1}$  ( $-\pi < \theta_{-1} < 0$ ), which are the angles separating the elastic sectors of the upper and lower half-planes from the plastic sectors. Stress variations and the angles separating the sectors in the upper half-plane are still governed by eqns (22) through (30), and those for the lower half-plane are given below. In sector (i) :

$$\begin{aligned} \sigma_{11} &= 2T_- + 2b_-(\theta + \pi) + b_- \sin 2\theta \\ \sigma_{22} &= 2b_-(\theta + \pi) - b_- \sin 2\theta \\ \sigma_{12} &= b_-(1 - \cos 2\theta). \end{aligned} \tag{32}$$

The intermediate parameter  $b_-$  in eqn (32) is determined from :

$$b_- = \frac{-2T_- \sin 2\theta_{-1} + \Delta_-}{4(1 - \cos 2\theta_{-1})} \quad \text{or} \quad \frac{-2T_- \sin 2\theta_{-1} - \Delta_-}{4(1 - \cos 2\theta_{-1})} \tag{33}$$

where

$$\Delta_- = \sqrt{8(1 - \cos 2\theta_{-1})k_-^2 - 4(1 - \cos 2\theta_{-1})^2 T_-^2}. \tag{34}$$

As in the case of  $b_+$ , the choice of  $b_-$  in eqn (33) should be made such that  $\sigma_{\text{eff}}$  is smaller than or equal to  $k_-$  for  $-\pi \leq \theta \leq \theta_{-1}$  and that  $|b_-/k_-|(1 - \cos 2\theta_{-1}) < 1$ . Stresses in sector (ii<sub>-</sub>) can be generated from those in eqn (32) by replacing  $\theta$  with  $\theta_{-1}$ .

In sector (iii<sub>-</sub>) :

$$\begin{aligned} \sigma_{11} &= T_- + 2b_-(\theta_{-1} + \pi) \pm k_-(2\theta_{-2} - 2\theta - \sin 2\theta) \\ \sigma_{22} &= T_- + 2b_-(\theta_{-1} + \pi) \pm k_-(2\theta_{-2} - 2\theta + \sin 2\theta) \\ \sigma_{12} &= \pm k_- \cos 2\theta. \end{aligned} \tag{35}$$

In sector (iv<sub>-</sub>) :

$$\begin{aligned} \sigma_{11} &= \sigma_{-0} - k_- \cos \eta_- \\ \sigma_{22} &= \sigma_{-0} + k_- \cos \eta_- \end{aligned}$$

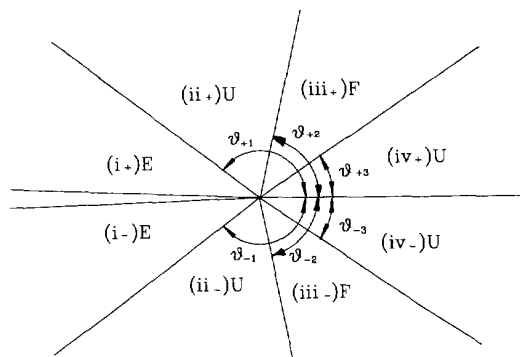


Fig. 12. An assembly of sectors around a ductile/ductile interface crack.

$$\sigma_{12} = k_- \sin \eta_- \tag{36}$$

where  $\sigma_{-0}$  is the (constant) mean stress in sector (iv<sub>-</sub>), which is given by

$$\sigma_{-0} = T_- + 2b_-(\theta_{-1} + \pi) \pm 2k_-(\theta_{-2} - \theta_{-3}). \tag{37}$$

The angle  $\theta_{-2}$  is obtained from the following two equations simultaneously :

$$\begin{aligned} \pm k_- \cos 2\theta_{-2} &= b_-(1 - \cos 2\theta_{-1}) \\ \pm k_- \sin 2\theta_{-2} &= -T_- - b_- \sin 2\theta_{-1} \end{aligned} \tag{38}$$

and the angle  $\theta_{-3}$  is given in terms  $\eta_-$  through

$$\theta_{-3} = -\eta_-/2 \pm \pi/4. \tag{39}$$

The unknown constants  $\eta_+(\pm\pi/2 - 2\theta_{+2} \leq \eta_+ \leq \pm\pi/2)$  and  $\eta_-(\pm\pi/2 \leq \eta_- \leq \pm\pi/2 - 2\theta_{-2})$  of the stress equations are not free parameters and must be determined from the following traction continuity equations at  $\theta = 0$ :

$$\begin{aligned} \sigma_{+0} + k_+ \cos \eta_+ &= \sigma_{-0} + k_- \cos \eta_- \\ k_+ \sin \eta_+ &= k_- \sin \eta_- \end{aligned} \tag{40}$$

where  $\sigma_{+0}$ , given in eqn (28), and  $\sigma_{-0}$ , in eqn (37), are indirectly dependent on, respectively,  $\eta_+$  and  $\eta_-$ . It is noted here that the + and - signs in the equations for each half-plane must be chosen independently and as part of the solution. Two representative solutions are shown below.

Shown in Fig. 13 is the case of a ductile bimaterial with  $k_+/k_- = 1.0/0.8$  and free parameters  $T_+ = 0.8$ ,  $T_- = 0.7$ ,  $\theta_{+1} = 150^\circ$ , and  $\theta_{-1} = -160^\circ$ , for which  $\eta_+ = -0.5010$  and  $\eta_- = -0.6440$  are obtained from eqn (40). The locations of the elastic sectors are indicated by the regions where the normalized effective stress  $\sigma_{eff}$  deviates from its constant yielding values. The stress variations seen in this example are representative of the mode I type solutions, as can be seen from their resemblance to those of the classic mode I slip-line field.

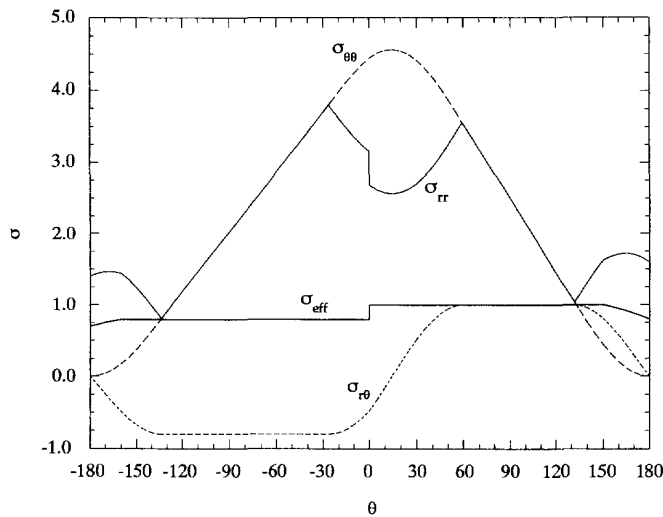


Fig. 13. Crack-tip angular stress variations for the assembly of sectors around a ductile/ductile interface crack shown in Fig. 12, normalized by  $k_+$ , with  $k_+/k_- = 1.0/0.8$ ,  $T_+ = 0.8$ ,  $T_- = 0.7$ ,  $\theta_{+1} = 150^\circ$ ,  $\theta_{-1} = -160^\circ$ .

A mixed-mode type solution is plotted in Fig. 14, which is for the case of a bimaterial with  $k_+/k_- = 1.0/0.5$  and free parameters  $T_+ = -0.8$ ,  $T_- = 0.4$ ,  $\theta_{+1} = 120^\circ$ , and  $\theta_{-1} = -160^\circ$ , from which it is found that  $\eta_+ = -0.1781$  and  $\eta_- = -0.3622$ . This solution differs from the previous one in that the normal stress along the crack flank is positive in one material and negative in the other, which is typical of the mixed-mode slip-line solutions for cracks in homogeneous, ideally plastic solids [see Dong and Pan (1990), and again notice the differences in the normalization of the stresses and in the definition of the effective stress  $\sigma_{\text{eff}}$ ].

#### SUMMARY AND CLOSING COMMENTS

The asymptotic near-tip stress field around stationary interfacial cracks has been investigated for ductile/rigid and ductile/ductile bimaterial interfaces under plane strain conditions, where the ductile materials are taken to be ideally plastic and incompressible and obey the von Mises yield criterion and the associated flow rule. Admissible solutions for the crack-tip stress field are obtained by assembling plastic as well as elastic sectors around the crack tip such that the traction-free conditions along the crack faces and the traction continuity conditions across the interface are satisfied simultaneously.

For ductile/rigid interfaces, crack-tip assemblies of sectors complementary to those by Guo and Keer (1990) and Zywicki and Parks (1992) are proposed. Several one-parameter families of solutions of the crack-tip stress field have been generated. These solutions possess features that resemble those found in the classic mode I and mode II slip-line fields.

For ductile/ductile interfaces, three assemblies are studied. When the interface crack is surrounded by plastic sectors only, only isolated mode I type solutions are found. When an elastic sector is present along the crack flank in one of the two ductile materials, a two-parameter family of solutions exists, which gives rise to both mode I type and mixed-mode type crack-tip stress fields. When two elastic sectors appear along the crack flank, with one in each ductile material, a four-parameter family of solutions can be found, which also gives rise to both mode I type and mixed-mode type crack-tip stress fields.

Before closing, it is worth pointing out that the stress field solutions constructed in this paper are only *statistically admissible*, although they are deemed, based on available information from the literature, most likely to exist for the interfacial crack problems studied. As such, this study does not tell which stress field can actually be achieved at the crack tip, resulting in some uncertainty about the solutions. It is expected that a more complete understanding of the crack-tip fields can be obtained by combining the result of

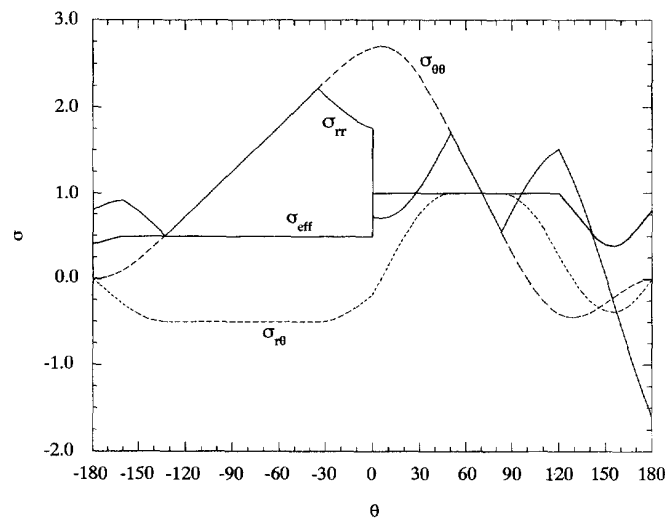


Fig. 14. Crack-tip angular stress variations for the assembly of sectors around a ductile/ductile interface crack shown in Fig. 12, normalized by  $k_+$ , with  $k_+/k_- = 1.0/0.5$ ,  $T_+ = -0.8$ ,  $T_- = 0.4$ ,  $\theta_{+1} = 120^\circ$ ,  $\theta_{-1} = -160^\circ$ .

this study with proper kinematic considerations, either asymptotically or in a full-field scale. For stationary cracks in elastic-perfectly plastic materials, however, asymptotic kinematical analysis is traditionally difficult and usually does not generate complete information for the crack-tip fields. It is felt then that a comprehensive finite element investigation can better serve the purpose. In order not to miss the possibility of loading-mode dependent crack-tip fields, it seems that a sufficiently wide range of loading cases need be studied. The stress fields presented in this paper can thus provide an important and necessary basis for the interpretation of the finite element results.

*Acknowledgements*—The author would like to thank Dr Michael A. Sutton and the anonymous reviewers for their discussions and constructive comments. This work was supported in part by a research start-up grant from the College of Engineering of the University of South Carolina, Columbia, S.C., and by a grant from the University of South Carolina Research and Productive Scholarship Fund.

#### REFERENCES

- Aravas, N. and Sharma, S. M. (1991). An elastoplastic analysis of the interface crack with contact zones. *J. Mech. Phys. Solids* **39**, 311–344.
- Champion, C. R. and Atkinson, C. (1990). A mode III crack at the interface between two nonlinear materials. *Proc. R. Soc. Lond.* **A429**, 247–257.
- Champion, C. R. and Atkinson, C. (1991). A crack at the interface between two power-law materials under plane strain loading. *Proc. R. Soc. Lond.* **A432**, 547–553.
- Comninou, M. (1978). The interface crack in a shear field. *J. Appl. Mech.* **45**, 287–290.
- Deng, X. (1993). Dynamic crack growth along elastic-plastic interfaces. *Int. J. Solids Structures* **30**, 2937–2951.
- Dong, P. and Pan, J. (1990). Plane-strain mixed-mode near-tip fields in elastic perfectly plastic solids under small-scale yielding conditions. *Int. J. Fract.* **45**, 243–262.
- Drugan, W. J. (1991). Near-tip fields for quasi-static crack growth along a ductile-brittle interface. *J. Appl. Mech.* **58**, 111–119.
- Gao, Y. and Lou, Z. (1990). Mixed mode interface crack in a pure power-hardening bimaterial. *Int. J. Fract.* **43**, 241–256.
- Guo, Q. and Keer, L. M. (1990). A crack at the interface between an elastic-perfectly plastic solid and a rigid substrate. *J. Mech. Phys. Solids* **38**, 843–857.
- Hutchinson, J. W. and Suo, Z. (1992). Mixed mode cracking in layered materials. *Adv. Appl. Mech.* **29**, 63–191.
- Larsson, S. G. and Carlsson, A. J. (1973). Influence of non-singular stress terms and specimen geometry on small-scale yielding at crack tips in elastic-plastic materials. *J. Mech. Phys. Solids* **21**, 263–277.
- Ponte Castaneda, P. and Mataga, P. A. (1991). Stable crack growth along a brittle/ductile interface—I. Near-tip fields. *Int. J. Solids Structures* **22**, 105–133.
- Rice, J. R. (1982). Elastic-plastic crack growth. In *Mechanics of Solids* (Edited by H. G. Hopkins, and M. J. Sewell), pp. 539–562. Pergamon Press, Oxford.
- Rice, J. R. (1974). Limitations to the small scale yielding approximation for crack tip plasticity. *J. Mech. Phys. Solids* **22**, 17–26.
- Rice, J. R. and Tracey, D. M. (1973). Computational fracture mechanics. In *Numerical and Computer Methods in Structural Mechanics* (Edited by S. J. Fenves *et al.*), pp. 585–623. Academic Press, New York.
- Sharma, S. M. and Aravas, N. (1991). Plane stress elastoplastic solutions of interface cracks with contact zones. *Mech. Mater.* **12**, 147–163.
- Sharma, S. M. and Aravas, N. (1993). On the development of variable-separable asymptotic elastoplastic solutions for interfacial cracks. *Int. J. Solids Structures* **30**, 695–723.
- Shih, C. F. and Asaro, R. J. (1988). Elastic-plastic analysis of cracks on bimaterial interfaces: Part I—Small scale yielding. *J. Appl. Mech.* **55**, 299–316.
- Shih, C. F. and Asaro, R. J. (1989). Elastic-plastic analysis of cracks on bimaterial interfaces: Part II—Structure of small-scale yielding fields. *J. Appl. Mech.* **56**, 763–779.
- Wang, T. C. (1990). Elastic-plastic asymptotic fields for cracks on bimaterial interfaces. *Engng Fract. Mech.* **37**, 527–538.
- Zywicz, E. and Parks, D. M. (1990). Elastic-plastic analysis of frictionless contact at interfacial crack tips. *Int. J. Fract.* **42**, 129–143.
- Zywicz, E. and Parks, D. M. (1992). On small-scale yielding interfacial crack-tip fields. *J. Mech. Phys. Solids* **40**, 511–536.